

1 **Thermal and Magnetic Context of Central Brazil**
2 **Structures: A study of magnetic lineaments in the**
3 **central Trans-Brazilian Lineament (TBL) and adjacent**
4 **regions.**

5 **Suze Nei Pereira Guimarães^{1*}, Fábio Pinto Vieira^{1†} and Valiya Mannathal**
6 **Hamza^{1‡}**

7 ¹National Observatory (ON/MCTI), Department of Geophysics, Geothermal Laboratory (LabGeot/ON),
8 Rio de Janeiro, Brazil

9 **Key Points:**

- 10 • magnetic lineaments
11 • vertical derivative
12 • lineament spacing
13 • spectral analysis
14 • heat flow

*suze@on.br

†fabiovieira@on.br

‡hamza@on.br

Corresponding author: Suze Nei Pereira Guimarães, suze@on.br

15 **Abstract**

16 This paper reports on the progresses obtained through the analysis of thermomagnetic
17 features of the region between the southern part of Tocantins state and the northern part of
18 Goias state, in Central Brazil. For that, we made use of data collected through aeromagnetic
19 surveys. Techniques of shading applied to vertical derivative of Anomaly Magnetic Field
20 (AMF) have been used to identify magnetic lineaments. The depth estimates of these
21 structures were obtained by means of spectral Analysis of AMF (Centroid method). The
22 results reveal the existence of a set of near-linear magnetic features in the region between the
23 longitudes of 48°W and 51°W and between the latitudes of 12°S and 14°S . This is also an
24 area of moderate microseismic activity and recent studies indicate anomalous geothermal
25 conditions at the upper crust. However, direct evidences of the occurrence of magmatic
26 intrusions at shallow crustal levels are absent. We postulate the hypothesis that the features
27 identified as a result of aeromagnetic survey are indicative of fracture systems, thereby
28 enabling the flow of carbonic fluids observed at the region's thermal springs and transporting
29 geothermal heat.

30 **1 Introduction**

31 The heat present in crust layers is a natural geothermal energy resource whose practical
32 exploitation is becoming increasingly widespread, worldwide. Geothermal resources are seen
33 as an alternative source of clean and removable energy (Ozgener et al., 2007). Currently,
34 the use of this source of energy is economically viable only in sites with an accumulation of
35 geothermal fluids. Moreover, in the deepest crust, the great part of this geothermal energy
36 is trapped in solid rock matrices.

37 In this context, the extensive crustal segments have become attractive targets for ex-
38 ploitation of resources from hot and dry rocks or hot and humid rocks types (Potter et al.,
39 1974). There is evidence of geothermal sources and heat anomaly map by heat flow distri-
40 bution in Trans-Brazilian lineament (TBL) region (Schobbenhaus, 1975). The geothermal
41 activity evidences the potential to be used directly as thermal springs or even indirectly as
42 the generation of electricity.

43 Aeromagnetic surveys have been employed in several studies of geologic provinces in
44 central Brazil. The focus of most of these investigations has been the mineral and hydrocar-
45 bon exploitation at shallow depths, in the upper crust. Very few attempts have been made
46 in using aeromagnetic data to explore crustal structures at deeper levels. (S. Guimarães et
47 al., 2014) employed spectral analysis techniques of aeromagnetic data in the understand-
48 ing of vertical distribution of magnetization in deeper crustal layers. This approach has
49 recently been used in the study of magnetized crustal blocks in the adjacent cratonic region
50 by (S. N. P. Guimarães & Hamza, 2019).

51 Geothermal resources of deep origin are generally related to magmatic intrusions (Kolstad
52 & McGetchin, 1978) positioned at varying levels of the crust. As a result, studies of the
53 crust's thermal field may be related to magnetometric investigations. In the present work,
54 we examine the vertical derivative of the anomaly magnetic field (AMF) by using shading
55 techniques (Blakely, 1996) in order to identify the magnetic lineaments in the study area
56 involving important geothermal environment, such as thermal springs. The depths of these
57 magnetic sources were inferred by spectral analysis of AMF.

58 The area under study is located in midwest region of Brazil cuted by the TBL, between
59 48°W and 51°W (longitude) and between of 12°S and 14°S (latitude).

60 2 Characterization of the Study Aea

61 The area of study comprise a parallelogram that includes the northern of Goiás state
62 and southern of Tocantins state, in central Brazil, Figure 1.

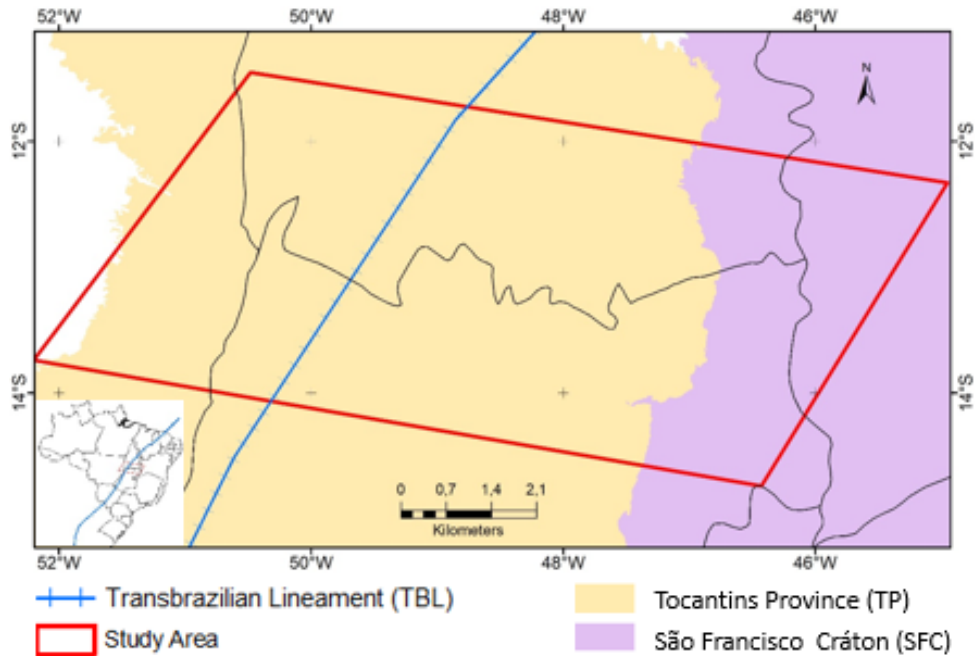


Figure 1: Location of study area.

63 The region lies on belts of phanerozoic covers (especially Brasília and Araguaia belts)
64 which feature geothermal anomalies, as observed in heat flow map of Brazil (Vieira, 2015).
65 The west part of this area is formed by the inner zone of Araguaia belt, Estrondo group and
66 the orthogneiss manifested as a result of the Brazilian Cycle. In the central part of the study
67 area lies part of Goiás Magmatic Arc and Goiás Massif which constitute important structural
68 sequences for this study. In the east part, the study area is limited by the Tocantins Province
69 (TP), characterised by the orthogneiss and greenstone belts of the Brasília belt and by the
70 São Francisco Craton (SFC), marked by the Bambuí group. The regional distribution of
71 these geological units are illustrated in the simplified geologic map of Figure 2.

72 Hot dry rocks in subsurface provide the ideal conditions of energy exploitation, due to
73 the extent of high fracturing degree at the crystalline basement. Pioneering studies of TBL
74 were carried out by (Schobbenhaus, 1975) and (de Brito Neves & Cordani, 1991). The deep
75 geothermal resources are generally related to magmatic intrusions positioned at varying
76 levels of the crust (3 to 10km) (Kolstad & McGetchin, 1978).

77 3 Data Acquisition and Methods

78 The aeromagnetic data used in this work is based on data sets compiled under the projects
79 designated as Brazil-Canada Geophysical (PGBC), Magmatic Arc Mara Rosa (MAMR -
80 Area 2), Paleo-Neoproterozoic of Northeast from Goiás (PNNG - Area 5), Tocantins (TO),
81 Complement of Tocantins (CTO) and Rio Formoso (RF). These are public domain data
82 sets, made available by CPRM for academic research purposes are illustrated in the Figure
83 3.

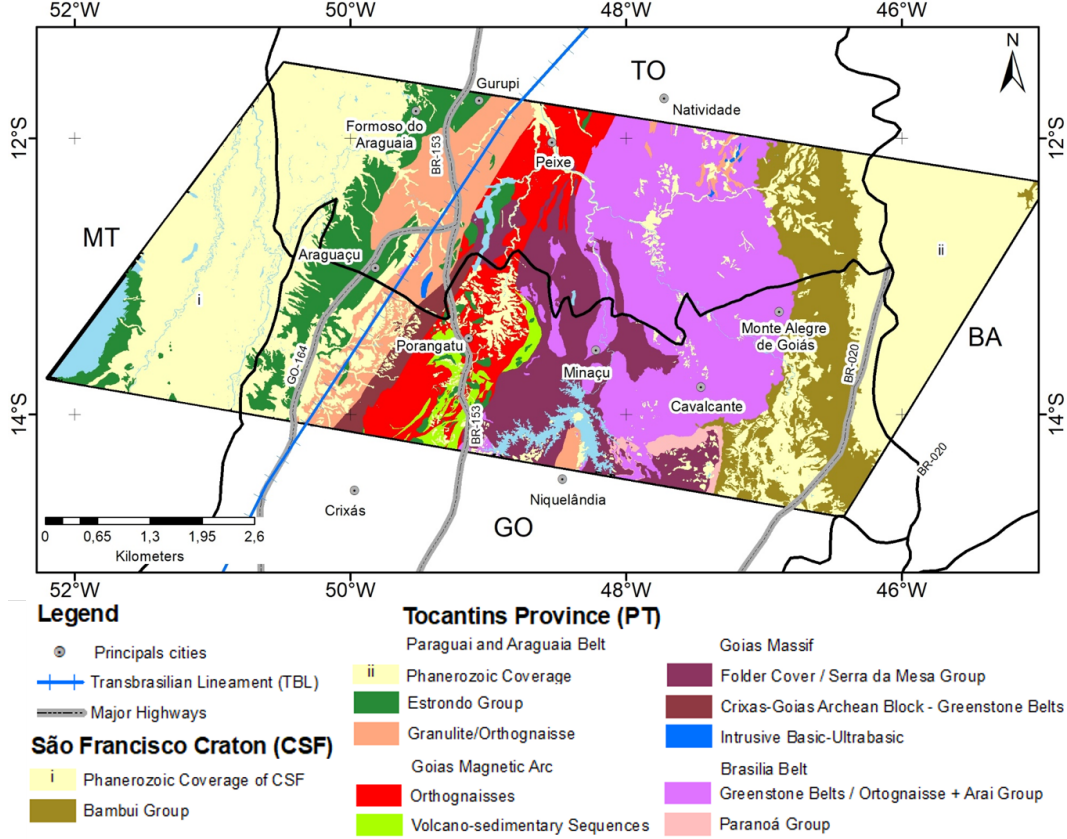


Figure 2: Simplified Geology Map of the study area (Modified from (CPRM, 2014))

84

The main characteristics of used data sets are described in Table 1.

85

86

87

88

89

90

91

92

93

94

Different types of processing techniques were applied on both types of database. For PGBC data, corrections were made for levelling, micro-levelling and filtering. These were followed by the removal of geomagnetic field components (diurnal and principal - IGRF), which allowed derivation of the residual or anomalous field. For data collected after the year 2000, the AMF was acquired with all corrections and levelling applied. Then, suture techniques were employed to generate a unified dataset. The degree of coherence this union was verified by the application of directional filters. The AMF map is illustrated in Figure 4, the parallelogram is a segment selected for the analysis of lineaments is also indicated, the blank areas on the polygon study indicating regions that have not been contemplated by the datasets.

95

3.1 Vertical Derivative of Crustal Magnetic Field

96

97

98

99

This is a processing technique for enhancing the high frequency of the magnetic signal where the magnetic anomaly is linearly transformed by means of the first derivative of the vertical component (z) of the AMF (\vec{B}), i.e., the vertical derivative measures the variation of the AMF with the vertical distance of source (Blakely, 1996).

100

In Fourier domain, it is defined by:

$$\mathfrak{F}\left(\frac{\delta^n B}{\delta z^n}\right) = |k|^n \mathfrak{F}[B] \quad (1)$$

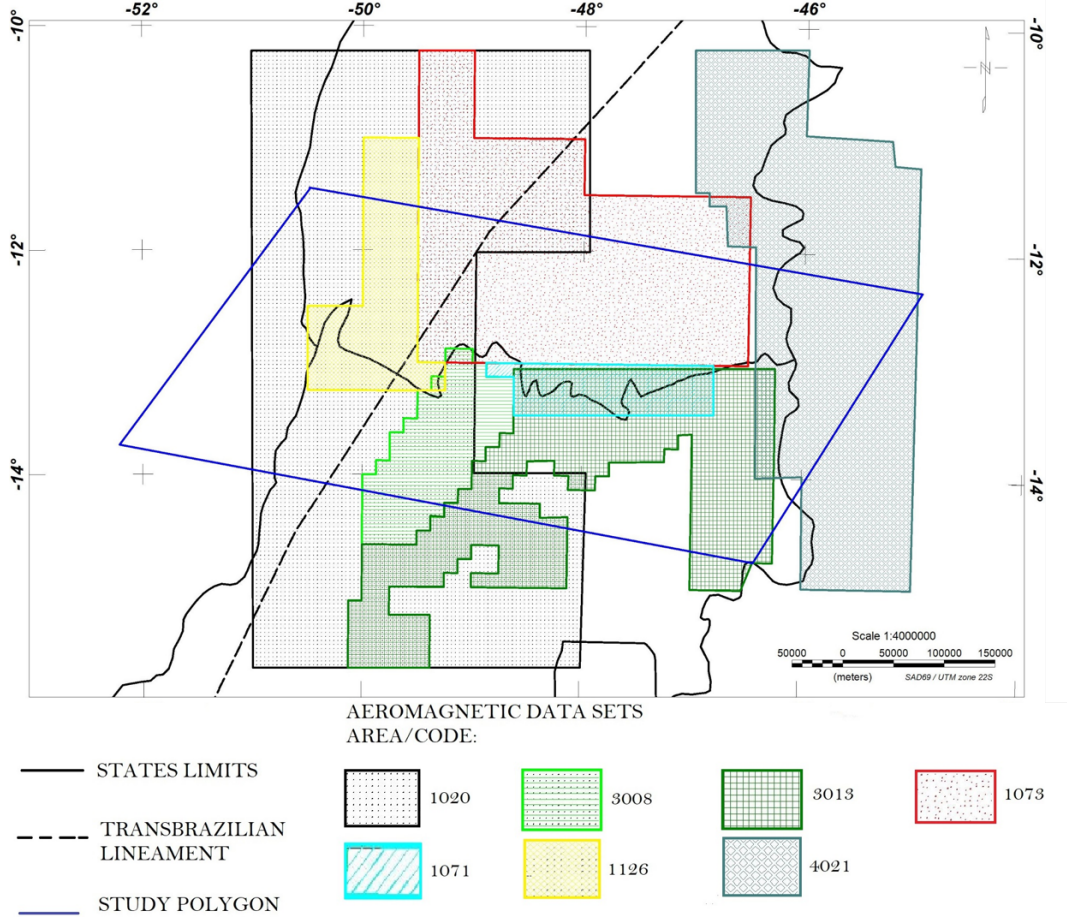


Figure 3: Areas of aerogeophysical projects used in this work.

$$k = \sqrt{(k_x)^2 + (k_y)^2} \quad (2)$$

101 The vertical derivative map enables a more detailed visualisation of the magnetic con-
 102 trast identified by the AMF, thereby allowing a better observation of the fault system and
 103 tectonic events. It is physically equivalent to the measurements of the magnetic field at two
 104 very close points, and the calculation is worked out by the quotient between the subtraction
 105 of these two points of magnetic field by their vertical separation. When applied to the mag-
 106 netic data of the AMF, the derivatives highlight the magnetic response of the more shallow
 107 geological bodies such as lineaments to the detriment of the deeper ones. Such a technique
 108 also assists the separation of anomaly Curves which may have been laterally superimposed.

109 In most cases, the features resulting from the application of this method appear as
 110 'ridges', whose geographical distribution occurs along lines, thus constituting so-called mag-
 111 netic lineaments. The mechanisms responsible for the connectivity of the magnetic linea-
 112 ments are believed to be alterations in the magnetic properties and also brittle behaviour of
 113 geological formations resulting from the action of local tectonic forces (Costa et al., 1985)
 114 (Osako et al., 1999). In the former, changes in the direction of lineaments represent changes
 115 in lithotypes. In the latter, the locations of changes in the direction of lineaments represent
 116 the local fracture zones. In the present investigation, vertical derivative techniques were
 117 applied by using Geosoft Oasis Montaj package (2019).

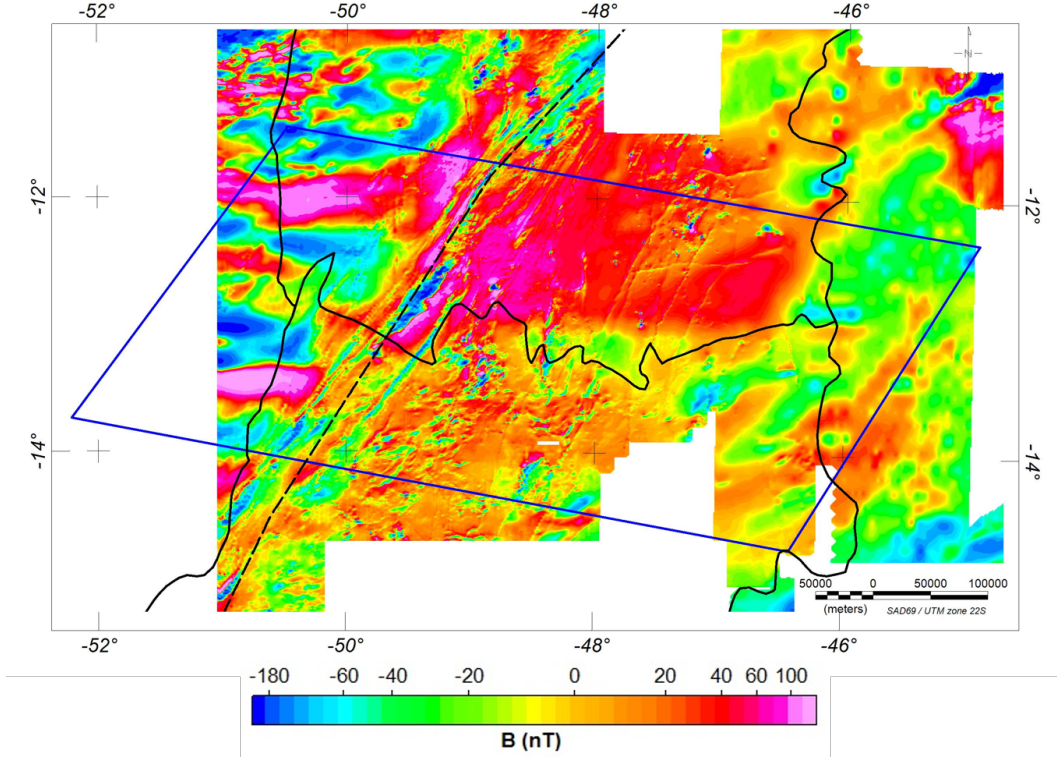


Figure 4: Crustal Magnetic Field Map in the study area.

3.2 Spectral Analysis of Crustal Magnetic Field

118

119 In order to determine the depth of magnetic sources in the subsurface, the spectral
 120 analysis technique used was the Centroid method (Bhattacharyya & Leu, 1977; Tanaka et
 121 al., 1999; Okubo et al., 1985). This method was initially based on the spectral tilt method
 122 proposed initially by (Spector & Grant, 1970). Both methods are based on the assumption
 123 that the anomalies observed in the AMF are produced by a distributed set of prismatic
 124 bodies. Assuming that these sets of magnetic sources form a semi-infinite layer and that
 125 their magnetization is a constant value, the Spector and Grant equation (1970) under the
 126 Blakely notation (1995), can be simplified as:

$$|F(k)|^2 = 4\pi^2 C_m^2 |\theta_m|^2 M_0^2 e^{-2kz_t} * \left(1 - e^{-k(z_b - z_t)}\right)^2 S^2(a, b) \quad (3)$$

127 where k is the wavenumber (cycles/km), C_m a constant, θ_m an angle related to the
 128 magnetization direction and θ_f an angle related to principal magnetic field direction in the
 129 final phase of acquisition data. M_0 is the magnitude of the magnetization vector, z_t and z_b
 130 are the top and bottom depths of magnetic sources. $S^2(a, b)$ is a factor related to horizontal
 131 dimensions of the anomalous magnetic source.

132 Therefore, the slope of the adjusted lines over the logarithm of the azimuth average
 133 power spectrum generated by a set of anomalous magnetic sources is related to the depth
 134 of the top of this set and also these spectra can relate a peak frequency (or wave number)
 135 to the thickness of the original magnetic layer.

136 In the Centroid method, the model is centred on collections of random samples of a
 137 uniformed distribution of prisms with constant magnetization. Thus, equation 3 is adjusted

138 in terms that involve z_t and z_b in a hyperbolic sine function, plus a centroid factor and for
 139 long wavelengths, the hyperbolic sine function tends to one, leaving only the centroid term,
 140 thus:

$$|F(k)|^2 \sim C e^{-kz_0} \Delta z k \quad (4)$$

141 In the methods proposed by (Bhattacharyya & Leu, 1977) and (Okubo et al., 1985),
 142 the estimates of the depth of the centroid (z_0) are obtained from the slopes of azimuthally
 143 averaged and the wavenumber scaled Fourier spectra in the low wavenumber region following
 144 the relation:

$$G(k) = \frac{1}{k} F(k) \quad (5)$$

145 Once the depth of the top of the deepest layer (z_t) is estimated from the amplitude
 146 spectrum, it is fairly simple to use the scaled amplitude spectrum to estimate the centroid
 147 depth (z_0). The bottom depth (z_b) is then obtained using the equation 6:

$$z_b = 2z_0 - z_t \quad (6)$$

148 The spectral analysis programme (routine in MATLAB) utilized enables changes in size
 149 of search windows, allowing calculation of the depth of magnetic sources in different parts
 150 of the study area.

151 4 Results and Discussion

152 4.1 Analysis of Vertical Derivative

153 The study of magnetic expressions of tectonic lineaments takes the enhancement of short
 154 wavelength anomalies. This is, on the whole, achieved by examining vertical derivatives of
 155 the AMF. Whence, maps of vertical derivatives are often employed in outlining tectonic lin-
 156 eaments. Magnetic imprints of lineaments arise from emplacement of thin sheets of material
 157 of relatively higher magnetic susceptibility. Fracture systems triggered by tectonic processes
 158 are responsible for the formation of a system of parallel fractures.

159 The study area involves two large-scale tectonic provinces: Tocantins Province (TP)
 160 that encloses the Trans-Brazilian lineament (TBL) on the western side and São Francisco
 161 Craton (SFC) on the eastern side. Analysis of the vertical derivative of the FMA indicated
 162 the presence of magnetic lineaments associated with TBL. These are closely-spaced linear
 163 magnetic features, as illustrated in Figure 5.

164 The cyan line in the map (Figure 5) is the lineament identified in previous geologic
 165 studies known as TBL. The magnetic lineaments were identified by adjusting lines connect-
 166 ing the darkest ridges on the vertical derivative Map. In the case, the red lines represent
 167 the near-linear features that have been considered as indicative of fracture zones in the
 168 basement rocks.

169 The greatest part of the magnetic lineaments, identified in subsurface by means of
 170 vertical derivative analysis, are around TBL, which shows that actually the TBL is a zone
 171 of lineaments with the same direction and characteristic of tectonics. It is evident from
 172 application of processing techniques that the dataset used in this study does not have a
 173 uniform resolution degree. In the vertical derivative this fact becomes patent in the SFC
 174 region and in the northwest region of study area. Hence, some lineaments were identified by
 175 cross-checking these with geologic information in order to increase the reliability in the data

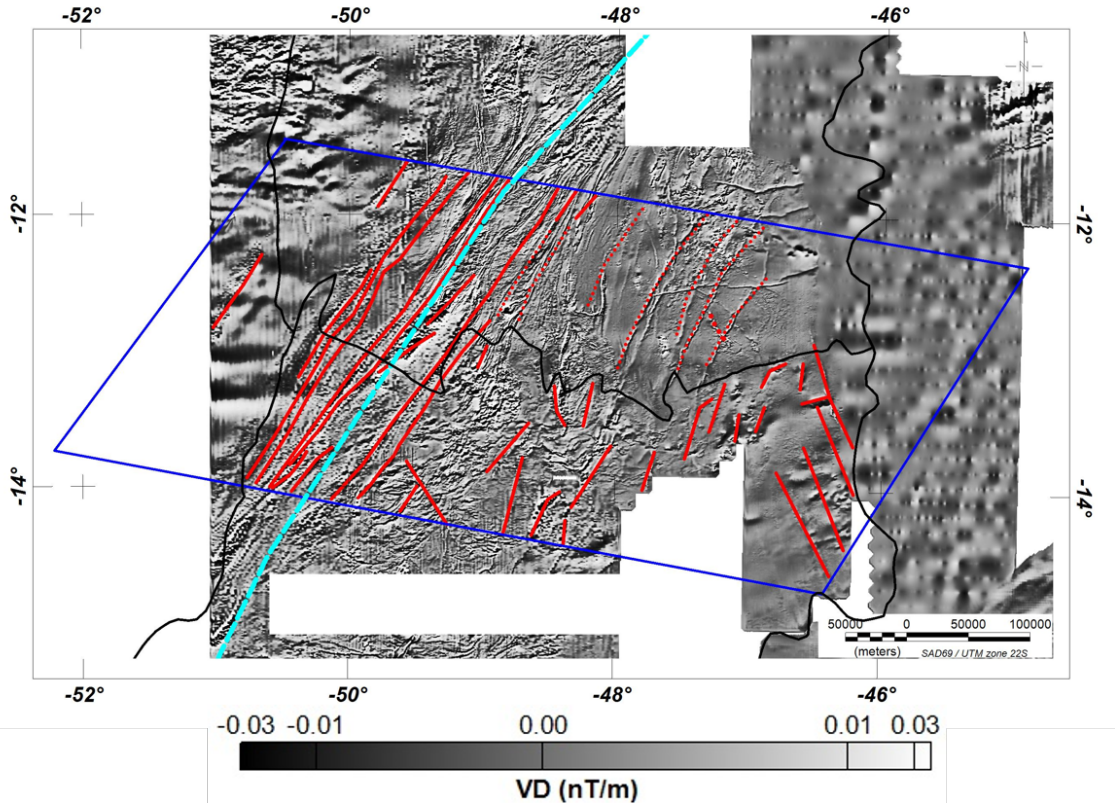


Figure 5: Distribution of Vertical Derivative of the Residual Magnetic Field in the study area. The red lines refer to mapping Magnetic Lineaments.

176 analysis. These lineaments are indicated in the map of Figure 5 as red-dotted lines. The
 177 blank segments in this map represent the areas deprived of the needed spectral resolution.

178 More than ten fracture zones with magnetic expressive ness can easily be identified in
 179 the vertical derivative map. These feature a NE-SW trending direction. Note that the lateral
 180 spacing (Figure 6), of such features is relatively small, ranging between 5 and 20 km, around
 181 TBL. The presence of such closely-spaced anomalies may be considered an indication that
 182 TBL in the study area is composed of a set of parallel quasi-linear fracture zones. Fracture
 183 zones are also observed in the region between TBL and SFC. Nonetheless, their spacing is
 184 relatively larger, of the order of tens of kilometres. The directions of these fracture zones
 185 are likewise NE-SW oriented, albeit in the north region a small change in the lineaments
 186 can be perceived to the E, while in the south part of the area, some lineaments feature a
 187 NW-SE direction.

188 According to (Gholipour et al., 2016) the differences in fracture spacing have been
 189 deemed as indications of fundamental differences in deep tectonic processes. It is also
 190 noteworthy that fracture zones are absent in the cratonic region on the eastern side of the
 191 study area. This may indicate that the cratonic area may be comprised of relatively unbroken
 192 structural elements with practically no significant contrast in their magnetic properties.

193 4.2 Deep Crustal Structure

194 The spectral analysis of the FMA obtained from aeromagnetic data was used as a
 195 means to infer depth values of subsurface anomalous magnetic sources, thus investigating

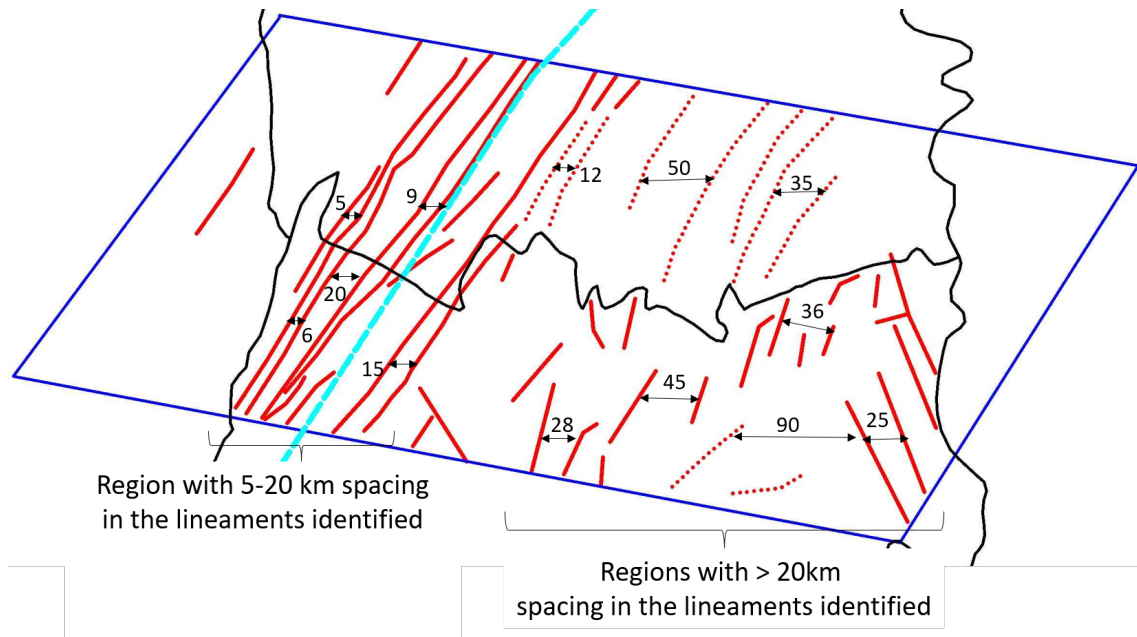


Figure 6: Fractures Spacing identified using Vertical Derivative techniques.

196 some fundamental points of the crust's thermal history in the given study area. As a
 197 consequence of data availability, three sizes of investigation window were employed, these
 198 being: 150km, 225km and 300km. The centroid method used in this study allows the
 199 identification of magnetized layers as per their wavenumber range, and consequently, three
 200 types of sources can be recognised: shallow, intermediate and deep. The results obtained
 201 through this method are presented in Table 2.

202 With the depth values for the magnetic layers acquired in the study area, the estimated
 203 value for Curie surface varies between 42 and 55km, with the shallow source layer limited
 204 to a 2-km depth. Figure 7 illustrates this subsurface arrangement of the magnetized crust
 205 or Curie surface.

206 Deep crustal structures of the study area may be assumed by considering vertical vari-
 207 ations in Moho depths, Curie temperatures and heat flow along selected profiles. The first
 208 profile (P1) has NE-SW direction, between the longitudes 50° W and 48° W and coincides
 209 with the TBL direction. It is situated in the western part of the study area. The second
 210 profile (P2) have a W-E direction cutting across the structural provinces of TP and SFC.
 211 The third profile (P3) have NE-SW direction, between the longitudes 47° W and 46° W and
 212 it is within the SFC. Values of Moho depths along the profiles are based on results reported
 213 by seismic studies of the region (Assumpção et al., 2013). Variations of Moho and Curie
 214 depths along the P2 are shown in Figure 8.

215 In this Figure 8, the top panel indicates variations in Moho and Curie depths, while the
 216 bottom panel illustrates heat flow variations (magenta curve). It is evident that there is a
 217 prominent heat flow anomaly in the region between TBL in TP and SFC. The variations of
 218 the Moho and Curie depths in the two others profiles listed above (P1 and P3) are illustrated
 219 in Figure 9 and Figure 10, respectively.

220 The P1 coincides with the TBL region mapped by (Schobbenhaus, 1975). In this profile
 221 region, the variations in Moho and Curie depths are much subdued. The heat flow in this
 222 region varies around $80\text{mW}/\text{m}^2$, which is considered high for Brazilian heat flow standards
 223 in view of its geological structure and rock age. In fact, in this region geothermal sources

Table 1: Main Characteristics of Airborne Geophysical Datasets used in this study.

	PGBC	MAMR	PNNG	TO	CTO	RF	SF
Code	1020	3008	3013	1073	1071	1126	4021
Acquisition Year	1976	2004	2006	2006	2007	2014	1980
Geophysical Information	Mag/ Gamma						
Line Spacing	2 Km	500 m					
Tie Spacing	14 Km	5 Km	5 Km	10 Km	10 Km	10 Km	12 Km
Line Direction	N-S						
Tie Direction	E-W						
Flight Height	150 m	100 m	125 m				
Range of Samples (mag/gamma)	1s	0.1/ 1.0s	0.1/ 1.0s	0.1/ 1.0s	0.1/ 1.0s	0.1/ 1.0s	0.1s

Table 2: Depth from top to bottom of Magnetic sources obtained in Spectral Analysis by Centroid Method, by investigation window size in the study area.

ID/ Windows (Km)	Long (W)	Lat (S)	Shallow	Intermediary	Deep
			Top/Bottom	Top/Bottom	Top/Bottom
M2 (300)	49.52	12.08	0.42	0.97	16.03
			0.83	3.67	33.30
M5 (225)	49.98	12.87	0.43	1.08	12.63
			0.87	5.77	28.28
M10 (150)	45.74	13.05	0.14	3.66	17.79
			1.88	6.76	32.79

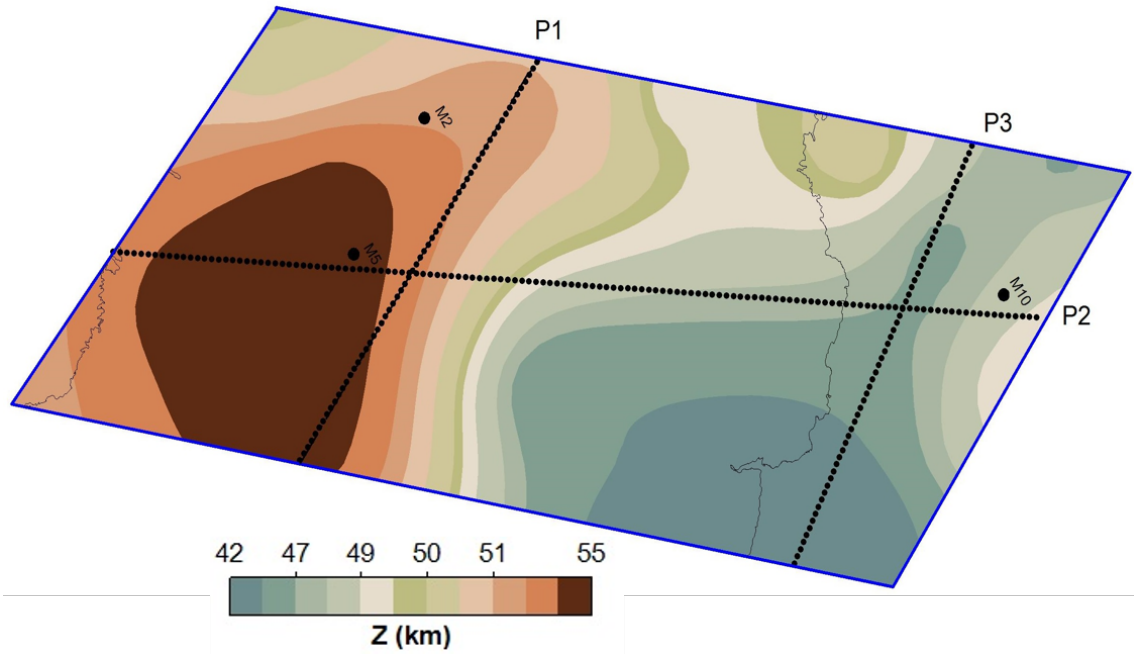


Figure 7: Depth of Magnetised Crust or Curie Surface using the deepest layers values from the Spectral Analysis. The dotted lines indicate the profiles selected for detail investigation.

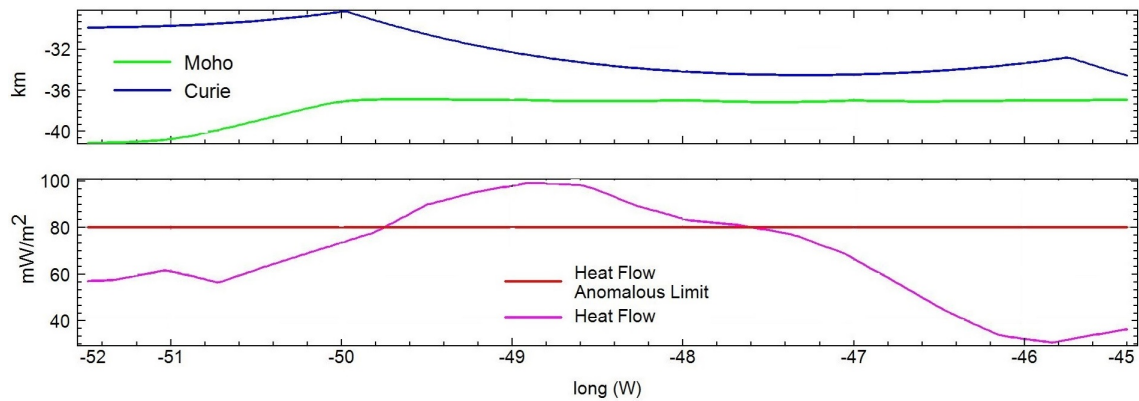


Figure 8: Lateral Variations in the Curie surface, Moho depth and Heat Flow along the Profile (P2) in the Central region, West-East (WE) direction of the study area.

224 that can be associated with the basement of the Paraguay belt and the magmatism of Goiás
 225 Magmatic Arc. The P3 is located at the SFC. The rocks that make up this area basement
 226 are very ancient and as a consequence, all the accumulated heat in the rock formation
 227 dissipated and the region is now considered geothermally cold. The values for heat flow
 228 in this profile are not greater than $50\text{mW}/\text{m}^2$. Additionally, it is evident that heat flow
 229 variations are much less subdued along the northern (P1) and southern (P3) parts of the
 230 study area. On one hand, both profiles (P1 and P2) bear the same crust depth compartment,
 231 where the Moho limits the magnetized crust (Curie surface), without evidencing any crust
 232 tuning. On the other hand, we can observe the outcrop geothermal sources in this region
 233 that demonstrate geothermal anomalies associated with tectonics and structural contexts.

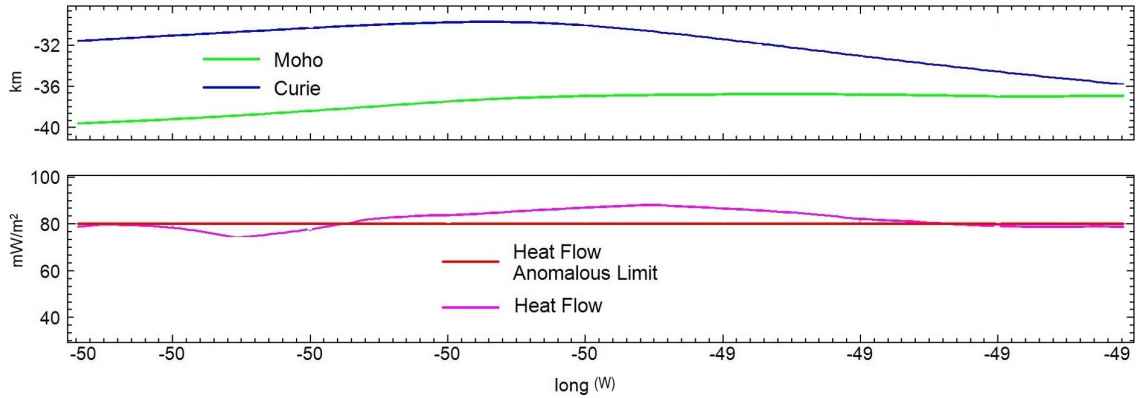


Figure 9: Lateral Variations in the Curie surface, Moho depth and Heat Flow along the Profile (P1) in the region of TBL, North-South (NS) direction of the study area.

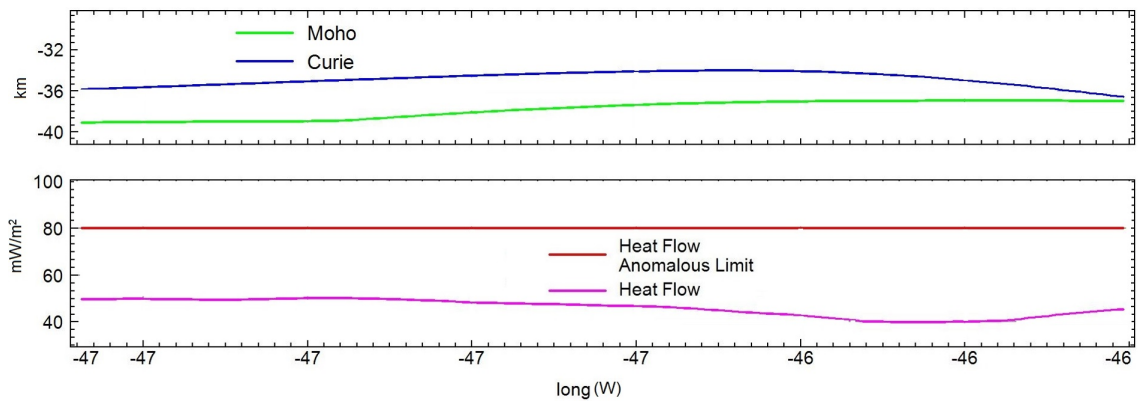


Figure 10: – Lateral Variations in the Curie surface, Moho depth and Heat Flow along the Profile (P3) in the region of SFC, North-South (NS) direction of the study area.

234

4.3 Spacing between Elements of the Lineament

235

236

237

238

239

240

Geologic lineaments are usually defined in literature as interpreted lines that have visible relations with geometrical features of terrain forms, such as valleys and slopes. A notable feature of the lineaments in Figure 4 is the high degree of parallelism between fracture zones. This is often taken as consequence of the thermomechanical nature of the rupture process in geological materials (Schultz & Fossen, 2008). The spacing between fracture zones can be measured in terms of the average distance between features in the lineament.

241

242

243

244

245

246

247

248

249

250

According to (Lamur, 2018) and (Lamur et al., 2017) changes in fracture spacing are produced by the upflow of hot material. In case of rapid upflow of high temperature molten magmatic material, the failure of confining rock strata takes place on a relatively short-time scale. The resulting fracture zone is an elongated feature with parallel sidewalls. Ergo, pulses of magma eruptions bring about sets of closely-spaced fracture zones. Similarly, in case of weaker effusive eruptions, internal pressure builds up on relatively longer time scales, producing fractures with larger Spacing. In brief, fracture spacing may indicate the type of fluid flows during the occurrence of lineaments. In this sense, effusive eruptions imply transport of geothermal heat by an upwelling flow of fluids rich in water or carbon dioxide (CO_2).

251 Hence, areas with wider fracture spacing are likely to be associated with localised heat
 252 flow anomalies. In the region of TP (involving TBL) the spacing of fracture zones is less than
 253 10km wide and several hundreds of kilometres long. These fracture zones feature a NE–SW
 254 trending direction. Contrastingly, in the region between TP and SFC the lateral spacing of
 255 fractures are relatively larger, ranging between 10km to 50 km.

256 4.4 Geothermal Field of the region between TBL and SFC

257 A recent geothermal study conducted by (Descovi & Vieira, 2019) has identified an
 258 anomalous geothermal field in the region between TBL and SFC. In this area, geothermal
 259 gradients vary from 15–55⁰C/km while thermal conductivity values are in the range between
 260 2.2–3.2 W/m.K. Consequently, heat flow values range from 40–160 mW/m². The heat flow
 261 map derived from the results obtained in the present work are illustrated in Figure 11.
 262 Therefrom, it can be inferred that heat flows in the region between TBL and SFC reach
 263 values in excess of 80 mW/m², in contrast to SFC, which has the lowest values of heat flow,
 264 to a great extent, smaller than 50 mW/m².

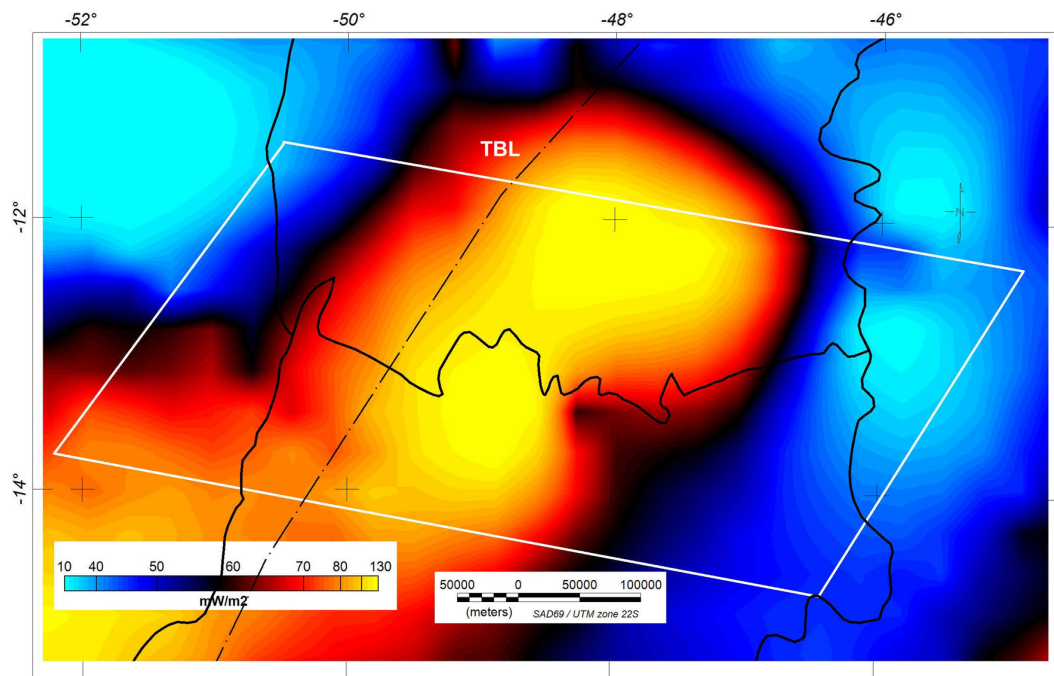


Figure 11: Heat Flow map of Northern Goiás and Southern Tocantins region between PT (involving TBL) and CSF.

265 It is clear that the anomalous geothermal conditions prevail in the region between TP
 266 and SFC in the northern parts of the Goiás state and southern parts of the Tocantins state.
 267 However, direct evidences of occurrence of magmatic intrusions at shallow crustal levels
 268 are absent. The great geothermal anomaly in this region can then be explained by the
 269 supplementary heat transport resulting from the ascending flow of carbonic fluids (Descovi
 270 & Vieira, 2019; Pinto-Coelho & Moura, 2016; Padilha et al., 2013; Abdallah, 2016; Solon et
 271 al., 2018) through the BR-19 quaternary fault (Porangatu fault zone).

272 5 Conclusions

273 Shading techniques applied to vertical derivative and spectral analysis of FMA have
 274 been used to identify and typify magnetic lineaments. The results obtained reveal the
 275 existence of a set of near-linear magnetic features in the region between 48°W and 51°W of
 276 longitude and between of 12°S and 14°S of latitude. Along the western side of the study
 277 area, the spacing of magnetic lineaments ranges between 5km to 10 km. Contrastingly,
 278 along the eastern segment of the study area, the spacing of fracture zones ranges from 10km
 279 to 50 km. This difference in the spacing of fracture zones has been considered an indicative
 280 of changes in the nature of deep-seated tectonic processes.

281 The magnetic sources depth inferred from the spectral analysis technique in the region
 282 spans from 35km to 50km. In the most part of the TP (involving TBL) region the thickness
 283 between the Curie and Moho surfaces differ in 10km. In the SFC region, this difference
 284 becomes almost null (2 km), evidencing that almost all the crust is magnetized.

285 The region between TP and SFC has moderate microseismic activity and recent studies
 286 point to anomalous geothermal conditions in the upper crust. However, direct evidences on
 287 the occurrence of magmatic intrusions at shallow crustal levels are absent. In the present
 288 work, we suggest the possibility that features identified in aeromagnetic datasets are indica-
 289 tive of fracture systems which made up-flows of carbonic fluids viable thereby transporting
 290 geothermal heat. The presence of flows of CO₂ has been observed at sites of thermal springs
 291 in the region.

292 Acknowledgments

293 The aeromagnetic database used in this research were provided by the Geological Service
 294 of Brazil (CPRM), being available on the platform <http://geosgb.cprm.gov.br/>, upon reg-
 295 istration on the website. SNPG also acknowledges the Post-Doctoral scholarship funded by
 296 PNP/CAPEF at Department of Geophysics at the National Observatory – ON/MCTIC.
 297 VMH also acknowledges the Productivity Research Fellowship provided by means of CNPq.

298 References

- 299 Abdallah, S. (2016). Geologia e geoquímica do grupo riachão do ouro na folha arraiaias:
 300 Evidências de arco magmático paleoproterozoico. *Geochimica Brasiliensis*, 29(2), 100–
 301 115.
- 302 Assumpção, M., Bianchi, M., Julià, J., Dias, F. L., França, G. S., Nascimento, R., . . . Lopes,
 303 A. E. (2013). Crustal thickness map of brazil: Data compilation and main features.
 304 *Journal of South American Earth Sciences*, 43, 74–85.
- 305 Bhattacharyya, B., & Leu, L.-K. (1977). Spectral analysis of gravity and magnetic anomalies
 306 due to rectangular prismatic bodies. *Geophysics*, 42(1), 41–50.
- 307 Blakely, R. J. (1996). *Potential theory in gravity and magnetic applications*. Cambridge
 308 university press.
- 309 Costa, P. d. O., Andrade, A. d., Lopes, G., & Souza, S. d. (1985). Projeto lagoa real-
 310 mapeamento geológico 1: 25.000. *Nuclebrás/CBPM, Salvador, Bahia*.
- 311 CPRM. (2014). *Database on line. fonte: www.cprm.gov.br/publique/geologia/geologia-
 312 basica/programa-geologia-do-brasil-pgb-79*.
- 313 de Brito Neves, B. B., & Cordani, U. G. (1991). Tectonic evolution of south america during
 314 the late proterozoic. *Precambrian Research*, 53(1-2), 23–40.
- 315 Descovi, P. L., & Vieira, F. P. (2019). Regions of anomalous geothermal fields in the state of
 316 tocantins, central brazil. *International Journal of Terrestrial Heat Flow and Applied
 317 Geothermics*, 2(1), 30–36.
- 318 Gholipour, A. M., Cosgrove, J. W., & Ala, M. (2016). New theoretical model for predicting
 319 and modelling fractures in folded fractured reservoirs. *Petroleum Geoscience*, 22(3),
 320 257–280.

- 321 Guimarães, S., Ravat, D., & Hamza, V. (2014). Combined use of the centroid and matched
 322 filtering spectral magnetic methods in determining thermomagnetic characteristics of
 323 the crust in the structural provinces of central brazil. *Tectonophysics*, *624*, 87–99.
- 324 Guimarães, S. N. P., & Hamza, V. M. (2019). Thermomagnetic features of pirapora region,
 325 central brazil. *International Journal of Terrestrial Heat Flow and Applied Geother-*
 326 *mics*, *2*(1), 22–29.
- 327 Kolstad, C., & McGetchin, T. (1978). Thermal evolution models for the valles caldera
 328 with reference to a hot-dry-rock geothermal experiment. *Journal of Volcanology and*
 329 *Geothermal Research*, *3*(1-2), 197–218.
- 330 Lamur, A. (2018). *Development, impact and longevity of fractures in magmatic, volcanic*
 331 *and geothermal systems* (Unpublished doctoral dissertation). University of Liverpool.
- 332 Lamur, A., Kendrick, J., Eggertsson, G., Wall, R., Ashworth, J., & Lavallée, Y. (2017).
 333 The permeability of fractured rocks in pressurised volcanic and geothermal systems.
 334 *Scientific reports*, *7*(1), 1–9.
- 335 Okubo, Y., Graf, R., Hansen, R., Ogawa, K., & Tsu, H. (1985). Curie point depths of the
 336 island of kyushu and surrounding areas, japan. *Geophysics*, *50*(3), 481–494.
- 337 Osako, L. S., et al. (1999). Estudo do potencial mineral do deposito uranifero de lagoa real,
 338 ba, com base em dados geologicos, aerogeofisicos e de sensoriamento remoto.
- 339 Ozgener, L., Hepbasli, A., & Dincer, I. (2007). Parametric study of the effect of reference
 340 state on energy and exergy efficiencies of geothermal district heating systems (gdhss):
 341 an application of the salihli gdhs in turkey. *Heat Transfer Engineering*, *28*(4), 357–
 342 364.
- 343 Padilha, A. L., Vitorello, I., & Pádua, M. B. (2013). Deep conductivity structure beneath
 344 the northern brasília belt, central brazil: Evidence for a neoproterozoic arc-continent
 345 collision. *Gondwana Research*, *23*(2), 748–758.
- 346 Pinto-Coelho, C. V., & Moura, M. A. (2016). Mineralizações de sn do maciço granítico serra
 347 branca, goiás: evolução do sistema hidrotermal e fonte dos fluidos. *Revista Brasileira*
 348 *de Geociências*, *36*(3), 513–522.
- 349 Potter, R., Robinson, E., & Smith, M. (1974, January 22). *Method of extracting heat from*
 350 *dry geothermal reservoirs*. Google Patents. (US Patent 3,786,858)
- 351 Schobbenhaus, C. (1975). *Carta geológica do brasil ao milionésimo: folha goiás (sd-22)*.
- 352 Schultz, R. A., & Fossen, H. (2008). Terminology for structural discontinuities. *AAPG*
 353 *bulletin*, *92*(7), 853–867.
- 354 Solon, F., Fontes, S., & La Terra, E. (2018). Electrical conductivity structure across the
 355 parnaíba basin, ne brazil. *Geological Society, London, Special Publications*, *472*(1),
 356 109–126.
- 357 Spector, A., & Grant, F. (1970). Statistical models for interpreting aeromagnetic data.
 358 *Geophysics*, *35*(2), 293–302.
- 359 Tanaka, A., Okubo, Y., & Matsubayashi, O. (1999). Curie point depth based on spectrum
 360 analysis of the magnetic anomaly data in east and southeast asia. *Tectonophysics*,
 361 *306*(3-4), 461–470.
- 362 Vieira, F. P. (2015). *Energia geotérmica de media e alta entalpia no brasil: Avaliações*
 363 *de recursos e perspectivas de aproveitamento (in portuguese)*. (Unpublished doctoral
 364 dissertation). Observatório Nacional / MCTI.